Many-particle effects in Be-δ-doped GaAs/Al_{x}Ga_{1-x}As quantum wells

Many-particle effects in Be-δ-doped GaAs/$Al_xGa_{1-x}As$ quantum wells

M. Kemerink, P. M. M. Thomassen, P. M. Koenraad, P. A. Bobbert, J. C. M. Henning, and J. H. Wolter
COBRA Interuniversity Research Institute, Eindhoven University of Technology, P.O. Box 513, NL-5600 MB Eindhoven, The Netherlands
(Received 17 October 1997)

We have performed photoluminescence (PL) and photoluminescence excitation measurements on two series of center-δ-doped p-type GaAs/$Al_xGa_{1-x}As$ quantum wells, with variable well width and doping concentration. The experimental data are compared with self-consistent field calculations. The effects of exchange and correlation were found to be extremely important and various models for the hole exchange and correlation are compared with the experimental data. It is found that the model recently proposed by Bobbert *et al.* [P. A. Bobbert *et al.*, Phys. Rev. B **56**, 3664 (1997)] consistently describes our experimental observations. Furthermore, for well widths $w \geqslant 600$ Å clear excitonic effects were observed, for hole densities as high as 12×10^{12} cm^{-2}, which is explained in terms of small spatial overlap between the screening particles and the exciton along the growth direction. In contrast to earlier work on similar samples, we found no indication for a Fermi-edge singularity in the PL spectra of our samples. Peaked structures at the high-energy side of the PL spectra are shown to arise from bulk transitions. [S0163-1829(98)04324-0]

I. INTRODUCTION

The collective behavior of mobile carriers in a semiconductor lattice has attracted a lot of attention ever since the early days of semiconductor physics. With the advent of (quasi-) two-dimensional (2D) systems, most of the many-body effects that had previously been studied in bulk semiconductors or metals became subjects of intense research in these structures. Among these are such well-known effects as screening, the Fermi-edge singularity (FES) or Mahan exciton, exchange and correlation, etc. Since exchange and correlation effects lead to a reduction of the effective band gap in degenerate systems, their effect is often denoted as band-gap renormalization (BGR). Although the basic concepts are not very new, all of these effects are still of great current interest.[1–4] Both experimental and theoretical studies on many-particle effects have predominantly focused on n-type systems, mainly to avoid the complications arising from the valence-band coupling. However, due to the very different characteristics of the valence bands as compared to those of the conduction band, i.e., the coexistence of heavy- and light-hole ground states, the high effective masses, and the strong nonparabolicity, the study of p-type systems can greatly enhance the general understanding of many-body physics.[5–10]

In this paper, we will report on photoluminescence (PL) and photoluminescence excitation (PLE) measurements on GaAs/$Al_{0.20}Ga_{0.80}As$ quantum wells (QW's) with a Be-δ-doping spike placed in the center of the well. These structures are ideal to study band-gap renormalization because of the high carrier densities that can be achieved, and the occupation of multiple subbands. We will compare our results with the results of self-consistent calculations, in which the effects of exchange and correlation have been incorporated by means of the local-density approximation (LDA). In particular, we will compare various models for the hole exchange-correlation potential with our experiments and calculations without these many-body corrections. We find that the inclusion of exchange and correlation effects in self-consistent calculations is essential for a meaningful comparison with experiments, and that the model that has recently been developed by Bobbert *et al.*[1] consistently describes our experimental findings.

In a recent series of papers, Wagner and co-workers[11–13] report the observation of a FES in the luminescence spectra of structures that are very similar to the ones discussed here. From a theoretical point of view this observation is very remarkable.[4,14,15] Both the small effective mass of the minority carriers and the large energetic separation between the highest occupied state and the lowest unoccupied state in the valence band, reported in Refs. 12 and 13, make the occurrence of a FES surprising. In our experiments, we do not observe any indication for a Fermi-edge singularity. In Sec. V we will briefly discuss this negative result in the light of recent theoretical work on this subject, and we will compare our results to those of Wagner and co-workers.

This paper is organized as follows. In Sec. II we will describe the samples used in this work. Experimental results will be reported in Sec. III and discussed in Sec. V. The numerical model used in the interpretation of our data is presented in Sec. IV, along with a comparison of measured and calculated transition energies. Section VI will summarize our conclusions.

II. SAMPLES

The structures investigated were grown on semi-insulating GaAs substrates by conventional molecular-beam-epitaxy techniques. On top of the substrate a 100-period GaAs/AlAs superlattice was grown, followed by a 200 Å $Al_{0.20}Ga_{0.80}As$ barrier layer. Both the superlattice and the $Al_{0.20}Ga_{0.80}As$ barrier were grown at 690 °C. Subsequently, the growth temperature was lowered to 480 °C to avoid Be diffusion during the growth of the active layers. The active layers consist of ten periods of the following structure: an undoped GaAs layer of width $w/2$, a Be-δ-doping spike with a Be surface concentration p, deposited during a growth interrupt, another undoped GaAs layer of width $w/2$, and a 75-

TABLE I. Growth parameters of the investigated samples. The Be-δ-doping spike is placed in the center of the GaAs well region. The confining $Al_{0.2}Ga_{0.8}As$ barriers are 75 Å thick.

Sample no.	Well width (Å)	Doping (10^{12} cm^{-2})
1	150	8
2	300	8
3	600	8
4	1200	8
5	600	2
6	600	4
7	600	12
Reference	2 μm	2×10^{18} cm^{-3}

Å $Al_{0.20}Ga_{0.80}As$ barrier. The total structure was terminated with another 125 Å of $Al_{0.20}Ga_{0.80}As$ and a 100 Å GaAs cap layer. In addition, a bulk Be-doped reference sample was grown. This structure consists of a single, 2 μm-thick bulk GaAs layer that had an aimed doping concentration of 2×10^{18} cm^{-3}. It was grown at 630 °C directly on top of a semi-insulating GaAs substrate.

The motivation for growing a multiple quantum-well structure, instead of a single QW, which is expected to show less broadened optical spectra, is twofold. Apart from the obvious increase in signal strength, two points are worth some further discussion. First, the two outer δ-doped wells will screen possible depletion fields, arising from mid-gap pinning of the Fermi level at the surface and in the substrate.[16] Therefore, the larger central part of the total structure will be unaffected by these uncontrollable fields, and thus will have a symmetric potential profile. This symmetry is essential in calculating the self-consistent solution of the coupled Poisson and Schrödinger equations. Furthermore, it has been shown by Rodriguez and Tejedor[4] that the symmetry of the confining potential can strongly affect the appearance of Fermi-edge singularities. Also for this reason, uncontrollable and possibly illumination-dependent electric fields are undesirable. Second, since the surroundings of the active layers are screened by the two outer wells, the Fermi level in the central eight wells is solely determined by the doping in the δ layers. The small (p type) background doping concentration in the order of a few times 10^{14} cm^{-3}, resulting from contaminations in the molecular-beam-epitaxy system, is fully negligible with respect to the amount of doping in the δ layers. This also facilitates numerical simulations, as it allows for a restriction of the calculation interval to the active layers. Furthermore, as δ-doped samples are not expected to show very sharp optical lines, some broadening due to fluctuations over the ten periods of active layers is acceptable.

Two series of δ-doped samples were grown. One with a variable doping concentration p, ranging from 2 to 12 $\times10^{12}$ cm^{-2}, at a fixed well width $w=600$ Å, and one with a variable well width, in between 150 and 1200 Å, at a doping level of $p=8\times10^{12}$ cm^{-2}. In Table I the relevant growth parameters are listed. In Figs. 1(a)–1(c) (self-consistent potentials and wave functions of three representative structures are displayed. The model used for the calculations is described in Sec. IV.

III. EXPERIMENTAL RESULTS

The experiments described in this paper are performed with the sample mounted in a continuous-flow He cryostat, in which temperatures from 4 to 300 K can be reached. Unless stated otherwise, all reported data are taken at 5 K. The samples were excited using either a tunable Ti:sapphire laser,

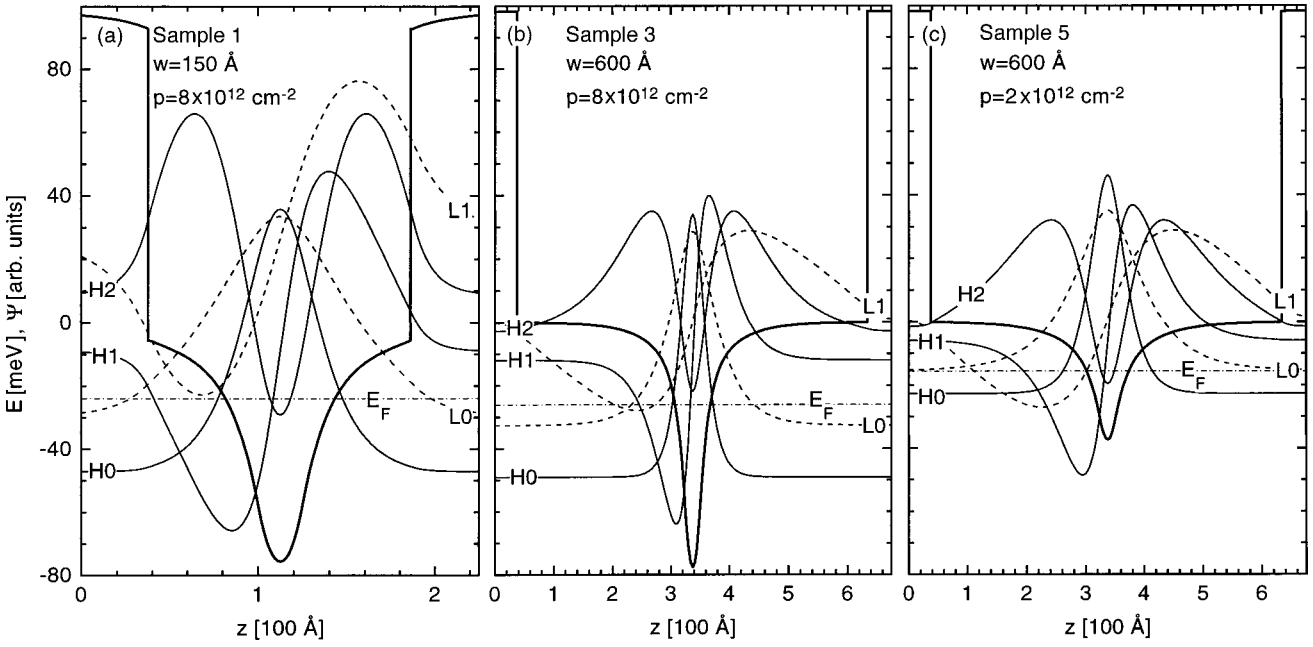

FIG. 1. Valence-band self-consistent confining potential and wave functions of samples 1 (a), 3 (b), and 5 (c), calculated using the model outlined in the text. The thick solid line denotes the confining potential, the thin solid and dashed lines denote the heavy- and light-hole envelope functions, respectively. The envelope functions are offset by their energy at $k=0$. The dash-dotted line indicates the position of the Fermi level E_F.

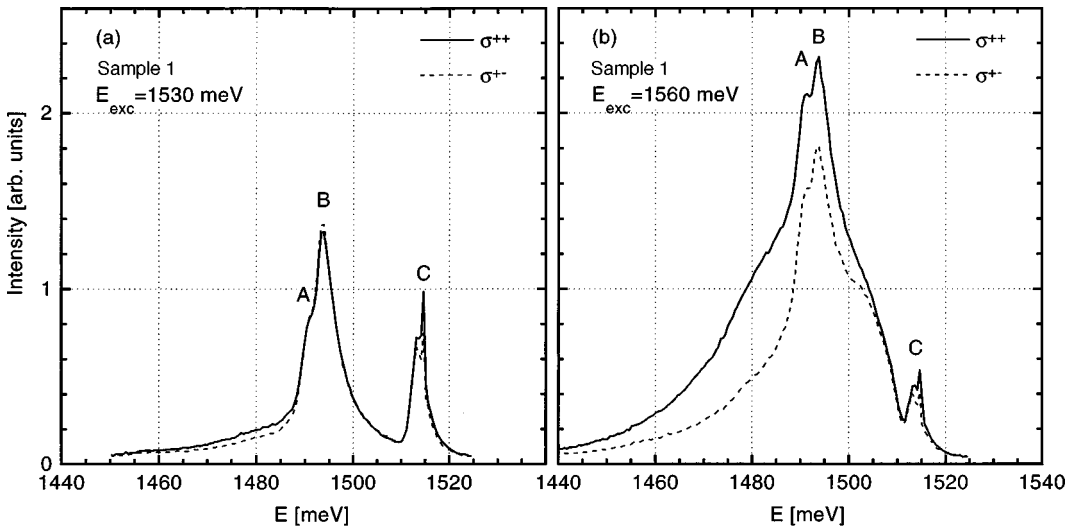

FIG. 2. Polarization-resolved photoluminescence spectra of sample 1, excited at 1530 meV [in the Moss-Burstein gap, panel (a)] and at 1560 meV [above the Moss-Burstein gap, panel (b)]. The solid and dashed lines are taken in parallel (σ^{++}) and cross (σ^{+-}) polarization configuration, respectively. The identification of peaks *A*, *B*, and *C* is discussed in the text.

or the yellow 594 nm (2.087 eV) line from a He–Ne laser. The former source excites below the band gap of the 20% $Al_xGa_{1-x}As$ barriers (1800 meV), the latter above. Both the excitation and detection beams were aligned perpendicular to the sample surface (backscattering configuration). Using polarization selective excitation and detection, i.e., using left (σ^-) or right (σ^+) circularly polarized light, heavy- and light-hole contributions to the optical spectra of the 2D structures could be separated. The excitation densities were approximately 1 and 0.15 W cm^{-2} for PL and PLE, respectively. The luminescence signal was dispersed by a double 0.75 m Spex monochromator and detected using a cooled GaAs photomultiplier, connected to a dc electrometer.

At the high-energy side of the PL spectra of all δ-doped samples, the structure appears to be independent of the well width and doping concentration. Also, the PLE spectra of these samples show a 2D structure-independent background signal, which is sensitive to the detection wavelength. We will first identify these structure independent features in the PL(E) spectra of the δ-doped samples as being due to bulk GaAs. Then, the 2D-related PL(E) spectra will be discussed.

A. Bulk-related PL(E)

Figure 2 displays the polarized luminescence spectra of sample 1 ($w=150$ Å, $p=8\times10^{12}$ cm^{-2}), taken with the exciting laser at 1530 meV (a) and 1560 meV (b). Both spectra exhibit the features labeled *A*, *B*, and *C* (at 1491, 1494, and 1513 meV, respectively), that, from their energetic position, can be identified as donor-acceptor (D,A), band-acceptor (e,A), and acceptor-bound exciton (A,X) recombinations in bulk GaAs, respectively. The identification of these features as being related to bulk transitions is confirmed by the following observations. First, as stated above, the lack of dependence on (2D) structural parameters. If one of the features were due to an enhancement of emission intensity at the Fermi level, or any other 2D-related transition, its position should definitely depend on the well width and doping concentration. Second, when exciting in the Moss-Burstein gap, i.e., at 1530 meV, see also Fig. 3, absorption in the 2D structure is forbidden due to the phase-space filling in the valence bands. No luminescence from the structure is therefore to be expected at this excitation energy. Third, the absence of polarization when the excitation is in the Moss-Burstein gap of the 2D structure is characteristic for bulk PL. When the PL signal of the wells is superimposed on the bulk lines, a polarized signal is to be expected, as is shown in Fig. 2(b). Fourth, Ferreira *et al.* demonstrated that for 150 Å wells with doping concentrations above $p=6\times10^{11}$ cm^{-2}, the bulk and 2D PL signals start to overlap.[6]

The excitation spectra of sample 1, detected either near the maximum of the bulk luminescence (1495 meV) or below the bulk PL (1480 meV), are shown in Figs. 3(a) and 3(b), respectively. Clearly, when the detection coincides with the bulk PL lines, three dominant lines are added to the excitation spectrum. The total disappearance of these lines when the detection is below the bulk PL indicates that, indeed, the emission features *A*, *B*, and *C* originate from a different region in the sample than the remainder of the luminescence. If this were not the case, carriers excited at any of the features *D*, *E*, or *F*, should be able to recombine at energies below feature *A*, i.e., in the quantum-well layers. Peaks *E* (1512 meV) and *F* (1516 meV) can now be identified as the absorption peaks of the acceptor bound and free excitons in bulk GaAs, respectively. The origin of structure *D* is not fully clear at present. From measurements with other detection energies we found that it is extended to, at least, 1485 meV, and that it is always of the same intensity as the *E* peak. It should be stressed that also the features *D*, *E*, and *F* are equally present in all samples.

B. 2D-related PL(E)

Polarization resolved PL and PLE spectra for samples 1, 3, and 5 are shown in Figs. 4(a)–4(c). The spectra of the other samples are fully consistent with the ones shown. The PL spectra are all taken using the Ti:sapphire laser as the excitation source. It is worthwhile to point out that none of

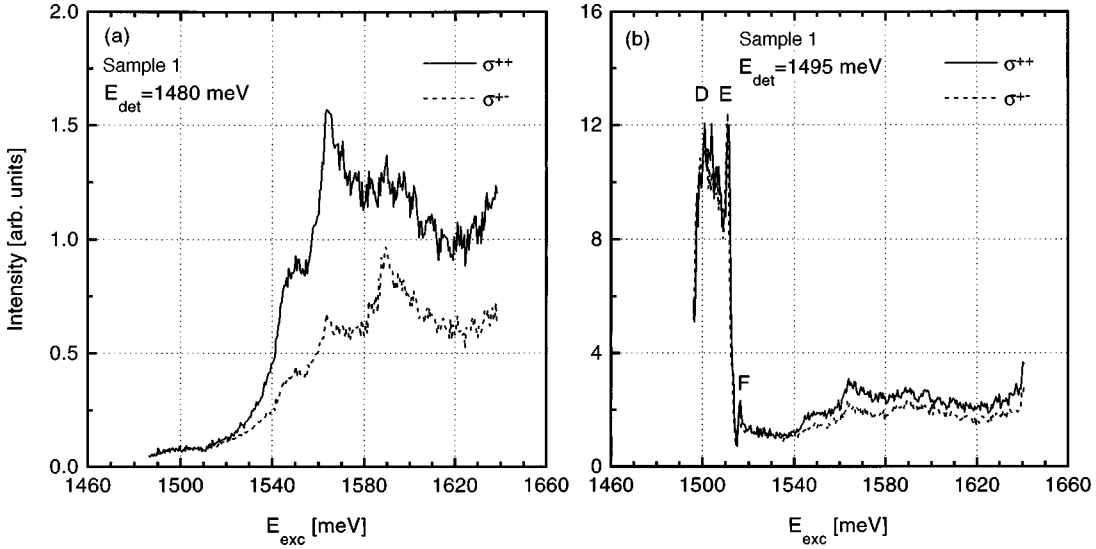

FIG. 3. Photoluminescence excitation spectra of sample 1, detected at 1480 meV (a) and at 1495 meV (b). The solid and dashed lines are taken in parallel (σ^{++}) and cross (σ^{+-}) polarization configuration, respectively. The identification of features D, E, and F is discussed in the text. The units of the vertical axis of the (a) and (b) panels are identical.

the PL spectra showed significant changes when the wavelength of the exciting light was changed, nor when the He-Ne laser was used for excitation, apart from an obvious scaling of the PL spectrum. This is in marked contrast with the observations in Refs. 11–13 where the appearance of a FES in the PL spectrum of similar structures is reported, once the photon energy of the exciting laser is above the band gap of the confining barriers. In Sec. V we will come back to this point.

From a comparison of the PL spectra of Figs. 4(a) and 4(b) it can be seen that the main effect of the increasing well width is a redshift of the 2D-related spectrum, due to the decreased confinement energy of the ground-state electron level $E0$. As the lowest light- and heavy-hole levels ($L0$ and $H0$) are solely confined by the notch potential of the δ-doping layer, see Fig. 1, their confinement energy is not expected to change significantly with increasing well width. This is reflected by the almost constant separation between the $H0$-$E0$ and $L0$-$E0$ luminescence lines, assumed to equal the separation between the positive and negative extrema in the polarization curve (dotted line). For the same reason, also the width of the PL line, reflecting the separation between $H0$ and E_F remains constant with increasing well width. Obviously, this is not the case when, at constant well width, the carrier density is decreased, as shown in Figs. 4(b) and 4(c). Here, the experiments indicate that the $L0$ subband is not significantly occupied, since the negative extremum in the polarization curve (σ^{++}-σ^{+-}) has disappeared, in agreement with our calculations (we calculate E_F-$L0$ $=0.6$ meV). The apparent blueshift with decreasing carrier density is due to the decreasing depth of the δ potential and the reduction of the strength of the exchange-correlation potentials with decreasing doping concentration, again in accordance with the calculations depicted in Fig. 1.

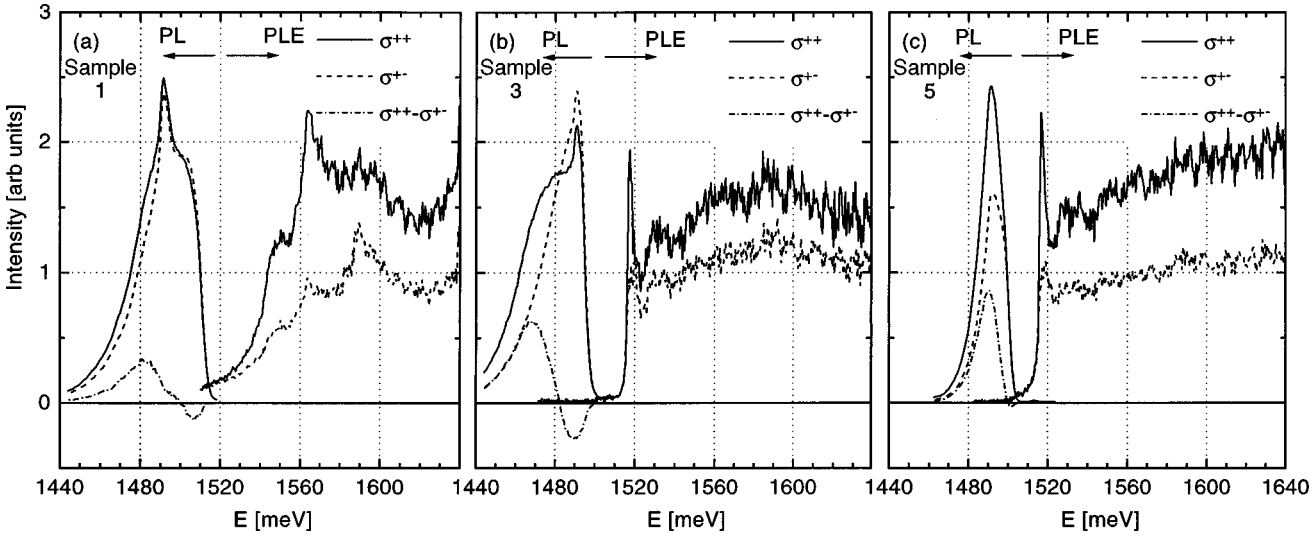

FIG. 4. PL and PLE spectra of samples 1 (a), 3 (b), and 5 (c). The PLE spectra are detected below the bulk PL signal. Solid and dashed lines denote σ^{++} and σ^{+-} polarizations, respectively. The dash-dotted line is the polarization curve, i.e., the difference between the polarized PL spectra.

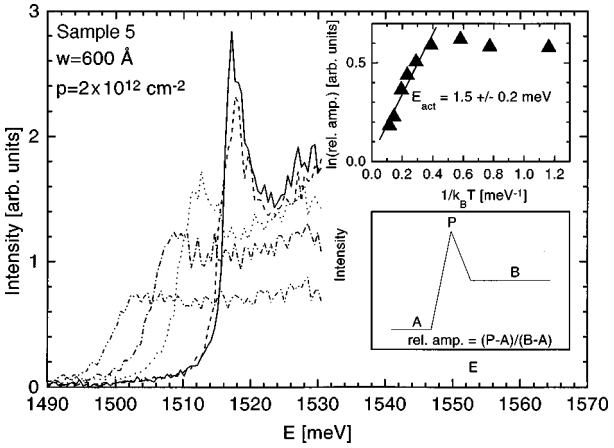

FIG. 5. (a) Main panel: The PLE onset of sample 5 in σ^{++} polarization at 20, 40, 60, 80, and 100 K. Upper inset: Activation plot of the normalized peak height. The activation energy of the exciton unbinding is 1.5 ± 0.2 meV. Lower inset: Schematic representation of the spectra plotted in the main panel and definition of the normalized peak height, used in the upper inset.

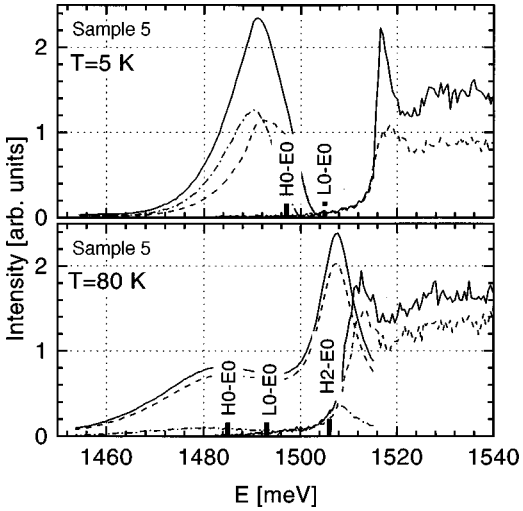

FIG. 6. PL spectra and PLE onsets at 5 and 80 K for sample 5. Note the strong line in the 80 K PL spectrum associated with $H2$-$E0$ recombination, which is visible due to the thermal population of the H2 subband. The thick vertical lines are calculated PL energies; the meaning of all other lines is the same as in Fig. 4.

The broad tail on the low-energy side of the PL spectra is assigned to transitions from background acceptor states to the lowest confined conduction-band level.[17] Since the energy gap between the acceptor level and the $E0$ level is dependent on the position of the acceptor in the well, the length of the low-energy tail is expected to correlate with the depth of the δ potential, i.e., with the doping concentration. Our measurements indeed show a monotonic increase of the tail length with increasing doping concentration, cf. Figs. 4(b) and 4(c). It is, however, extremely hard to quantify this effect, although the order of magnitude of the tail length compares favorably with the calculated potential profiles in Fig. 1.

The PLE spectra of our structures are hardly dependent on the doping concentration, as can be seen from a comparison of Figs. 4(b) and 4(c). This can easily be understood by realizing that the PLE spectrum is determined by the higher, unoccupied, hole levels and the empty electron levels. Since these states ''feel'' relatively little of the δ potential, they are hardly affected by an increase in the doping concentration, which only changes the central region of the notch potential. Although the $L0$ level seems unoccupied at a doping level of 2×10^{12} cm^{-2}, $L0$-$E0$ is not observable in the PLE spectrum, due to either the small matrix element for $L0$-$E0$ transitions (from calculations, the step at 1517 meV is expected to be a factor 3 higher than the $L0$-$E0$ absorption) or a small Moss-Burstein shift, resulting from a slight occupation of the $L0$ subband. Increasing, at constant-doping concentration, the well width from 150 to 600 Å, the steps at 1545 and 1565 meV [Fig. 4(a)] shift to lower energy, lose intensity, and seem to merge at 1518 meV [Fig. 4(b)]. Since these steps are due to $H2$-$E0$ and $H1$-$E1$ absorption, respectively, this behavior can be understood from two points. First, the obvious shifts of the hole and electrons with well width, which causes a strong reduction of the separation between these transitions. Second, the increasing well width causes a reduction of the $H1$-$E1$ matrix element by more than a factor 5, effectively removing the $H1$-$E1$ absorption step from the PLE spectrum. The step at 1527 meV in Fig. 4(b) is assigned to $H2$-$E2$ absorption.

Apart from the 150 and 300 Å samples (nos. 1 and 2), all samples show a sharp peak at the absorption onset. Based on its position and its small width (2.5 meV for sample 3), we assign this to a $H2$-$E0$ exciton. In order to validate this assignment, temperature-dependent PLE measurements were performed, see Fig. 5. The upper inset shows the activation plot of the height[18] of the excitonic PLE signal, normalized on the band-to-band PLE signal, as illustrated in the lower inset. The latter correction is needed to account for the temperature dependence of nonradiative losses that affect the PLE signal strength. Clearly visible is the activated behavior, with an activation energy of 1.5 ± 0.2 meV. Taking the large density of mobile carriers that screen the Coulomb interaction into account, this value seems reasonable.[19,8] In Sec. V this feature will be discussed in more detail.

Further confirmation of the assignment of the peak at the absorption onset to an excitonic transition of an unoccupied subband comes from the temperature dependence of the PL signal that is shown in Fig. 6. Clearly visible, apart from the redshift due to the shrinkage of the band gap with temperature, is the luminescence arising from one or more thermally occupied subbands. From our band-structure calculations we find for the $H1$-E_F, $H2$-E_F, and $E0$-$E1$ separations, respectively, 9.7, 14.1, and 3.9 meV. Comparing this to $k_BT = 7$ meV at 80 K, the assignment of this line to either $H1$-$E1$ or $H2$-$E0$ recombination is possible, since they have calculated transition energies of 1517 and 1518 meV, respectively. Since the matrix element for the $H2$-$E0$ transition in sample 5 is a factor 2 larger than for the $H1$-$E1$ transition, the former transition is expected to dominate. The coincidence of the PL maximum with the half-height point of the peak at the PLE onset shows that both peaks share the same origin.

IV. NUMERICAL CALCULATIONS

A. Model

The model used to obtain the self-consistent wave functions and confinement potentials of electrons and holes has

been described in detail in an earlier publication,[20] so only a brief outline will be given here. Additions that were made to the model described in Ref. 20, and that are essential for a proper calculation of the δ-potential solutions, will be discussed in more detail.

Hole wave functions and energies were obtained as numerically exact solutions of the 4×4 Luttinger Hamiltonian, including the valence-band anisotropy. The used Luttinger parameters are $\gamma_1=6.85$, $\gamma_2=2.1$, and $\gamma_3=2.9$ for GaAs and $\gamma_1=3.45$, $\gamma_2=0.68$, and $\gamma_3=1.29$ for AlAs,[21] the used electron masses in GaAs and AlAs are $0.067m_0$ and $0.15m_0$. The parameters for $Al_xGa_{1-x}As$ were calculated using the virtual-crystal approximation. The band gap of $Al_xGa_{1-x}As$ was calculated as $E_g(x)=1519.2+1360x+220x^2$ meV, where the common 40:60 rule was used for the distribution of the band-gap discontinuity over the valence and conduction bands at the GaAs/$Al_xGa_{1-x}As$ interfaces. The Hartree potential was calculated by solving the Poisson equation numerically. Only the ionized beryllium atoms and the occupied valence-band states are contributing to this potential, for reasons explained in Sec. II. The degree of ionization of the Be acceptors is assumed to be 100%.[22] The broadening of the Be δ layer is assumed to be rectangular, with a width of 25 Å.[12,23] In Ref. 23 it is shown by cleaved-edge scanning tunnel microscopy that Be-δ-doping layers in GaAs, grown under exactly the same circumstances as the present ones, have doping profiles with a full width at half maximum of about 10 Å, for doping concentrations up to 1×10^{13} cm^{-2}. We found that, within the experimental uncertainty, the calculated energy of all optical transitions is independent of the assumed broadening for widths up to 25 Å, which we used as a safe upper limit. In contrast to our experiences with barrier-doped p-type single and double QW's, it turned out that assuming parabolic valence bands in calculating the charge distribution gives erroneous results in these center-δ-doped wells. We therefore used the actual hole dispersions from the Luttinger Hamiltonian to calculate the Fermi level, and calculated the charge distribution by summing all (k dependent) hole wave functions up to the Fermi level. The density of states was used as weight function in the latter procedure. In order to expedite this part of the calculations, the axial approximation was applied in determining the Fermi level. In all other calculations the full warping was taken into account. Absorption spectra are calculated as indicated in Ref. 19.

For the structural parameters needed in the self-consistent calculations, i.e., the well width w and acceptor concentration p, the nominal values of the growth menu are taken. For the dopant concentration, the error made by this procedure can be estimated from the characterization data of the reference sample. This sample had a nominal Be concentration of 2×10^{14} cm^{-2} per μm GaAs; characterization with van de Pauw measurements showed an actual doping level of 1.97×10^{14} cm^{-2} per μm. The error in the subband calculations, caused by an error of this size in the dopant concentration, is fully negligible with respect to the experimental resolution. Deviations from the nominal value of the well width are usually a few percent. For 150 Å-wide wells this may cause measurable deviations in the calculations; for wider wells this will not pose a problem. It is important to note that no adjustable fitting parameters have been used in our model.

B. Exchange and correlation

Inclusion of many-particle corrections in the subband calculations beyond the direct Coulomb interaction or Hartree term turned out to be essential. In recent literature, various attempts have been made to capture the complications arising from the coexistence of light and heavy holes in calculations of the BGR in p-type systems.[24,25] Because of the high hole density and the occupation of multiple subbands, the present samples are extremely suited as a test system for various hole-BGR models. In this work, calculations based on the models proposed by Reboredo and Proetto[24] and Bobbert *et al.*[1] will be compared with calculations without exchange and correlation corrections, and with calculations based on the one-component plasma model of Hedin and Lundqvist.[26] The model proposed by Sipahi *et al.*[25] is only applicable to homogeneous systems, and can therefore not be applied to the present samples. However, as far as $k=0$ energies are concerned, this model is similar to the one proposed by Reboredo and Proetto, in the sense that holes with $|m_J|=\frac{3}{2}$ and $|m_J|=\frac{1}{2}$ experience different exchange-correlation corrections. For details concerning the various BGR models, the reader is referred to the original publications. However, for the sake of self-containedness, the basic assumptions of the models by Hedin and Lundqvist, Reboredo and Proetto, and Bobbert *et al.* will be briefly outlined below.

All three models apply the LDA for extending results obtained for a homogeneous bulk system to a quasi-2D system, by calculating an effective exchange-correlation potential V_{xc} that only depends on the local carrier density, i.e., $V_{xc}(p(z))$. The Hedin and Lundqvist model was originally derived for n-type systems. It therefore assumes that the carrier plasma consists of one type of (parabolic) carriers only. By applying this model directly to a hole gas, characterized by the effective heavy-hole mass m_h^*, one indirectly assumes that all holes are heavy holes. The validity of this assumption is further discussed in Sec. V. Although this assumption totally ignores the actual valence-band structure, favorable comparisons with experiments have been reported for BGR calculations that treat the valence bands as a single, parabolic band.[27–29] Since the Hedin-Lundquist model is only used for comparison with more sophisticated models, there is no particular reason for choosing this model instead of any other parametrized model available in the literature for calculating the BGR in n-type systems,[30,31] apart from the fact that the Hedin-Lundquist model appears to be the most popular. The model proposed by Reboredo and Proetto[24] is based on an analogy with the spin-density functional formalism. The exchange-correlation potential is made dependent on $|m_J|$, $V_{xc}^{|m_J|}(p^{3/2}(z),p^{1/2}(z))$. By ignoring exchange and correlation between light holes and heavy holes, the final exchange-correlation potential becomes only dependent on the local density of particles with $|m_J|=\frac{3}{2}$ or $\frac{1}{2}$, $V_{xc}^{|m_J|}(p^{|m_J|}(z))$. The quantity $p^{|m_J|}(z)$ is defined as the density in the heavy- ($|m_J|=\frac{3}{2}$) or light- ($|m_J|=\frac{1}{2}$) hole subbands. For the functions $V_{xc}^{|m_J|}$ a parametrized expression, derived for a one-component plasma, is used, where the carrier mass is chosen equal to an effective heavy- or light-hole mass, depending on $|m_J|$. To summarize, the most important feature of this model is that heavy and light holes experience

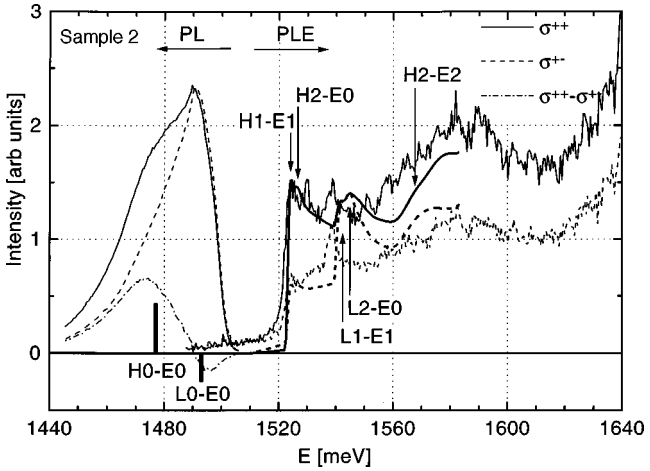

FIG. 7. Comparison between experimental and simulated PLE spectra of sample 2. The experimental PL spectrum can be compared with calculated transition energies for recombination at $k=0$ (thick vertical lines). Solid and dashed lines denote σ^{++} and σ^{+-} polarizations, respectively. The dash-dotted line is the difference between the polarized PL spectra. The thick, smooth lines are simulations, the thinner lines are experimental curves. The arrows identify the origin of features in the simulated PLE spectra.

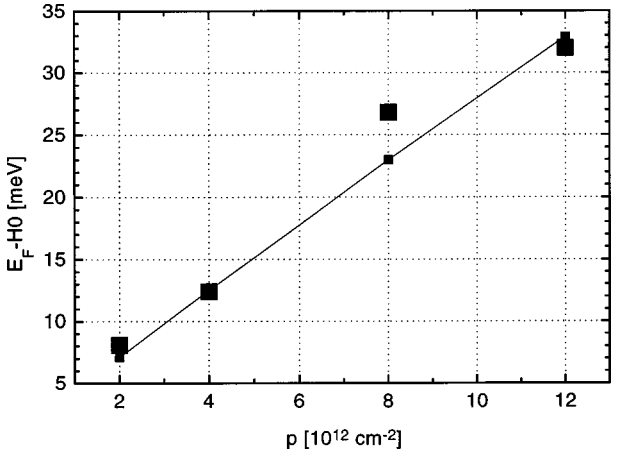

FIG. 8. Experimentally and numerically determined separation between the ground-state heavy-hole energy at $k=0$ and the Fermi energy versus doping concentration for $w=600$ Å. The large (small) squares denote experimental (numerical) points; the thin line connects the numerical points.

different exchange-correlation potentials. In Sec. V A, we will discuss the inconsistency and omissions of this model. The model derived by Bobbert *et al.* does not assign a particular character (heavy or light) or mass to individual subbands, as Ref. 24, or to particular spinor components, as Ref. 25, of the 2D structure. Rather, it is based on the notice that, within the LDA formalism, the quasi-2D structure *locally* is treated as *bulk* and that therefore the *bulk* dispersion relations must be used to determine the *local* amount of heavy and light holes. Based on this idea, Bobbert *et al.* calculate the exchange and correlation energy $\epsilon_{xc}(\rho)$ of a hole in a homogeneous hole gas of density ρ, where all heavy-hole–light-hole interactions, i.e., heavy-hole–heavy-hole, light-hole–light-hole, and heavy-hole–light-hole exchange and correlation, are taken into account. Since the Coulomb interaction is nondiagonal with respect to hole character, it is fundamentally impossible to identify a single hole as ''light'' or ''heavy.'' The exchange-correlation energy is therefore identical for all holes in the system. Subsequently, $\epsilon_{xc}(\rho)$ is converted to the exchange-correlation potential, using $V_{xc}(z)=-(d/d\rho)[\rho\epsilon_{xc}(\rho)](z)$. Note that also $V_{xc}(z)$ is equal for ''heavy''- and ''light''-hole subbands. Unless stated otherwise, all calculations shown are obtained using the model of Bobbert *et al.* for $V_{xc}(z)$.

To arrive at the total band-gap renormalization, also the correlation of the photogenerated electron with the sea of holes must be taken into account. Independent of the model used for the hole exchange-correlation potential, we use the parametrized expression of Ref. 1 for the electron-correlation potential $V_c(z)$, again using the LDA.

C. Numerical results

Because of the strong overlap of the electron and hole wave functions with the ionized acceptors, relaxation of the k-selection rules could easily result from localization or strong scattering. Before a meaningful comparison of experiments and calculations can be performed, it is therefore essential to determine whether or not the measured optical transitions are direct in k space. To do so, an experimental PL and PLE spectrum will be compared with numerical simulations, see Fig. 7. The numerical spectra (PLE) and energies (PL) are calculated with full k conservation. The good agreement between measured and calculated PLE spectra, both in position and steepness of onsets, shows that the relaxation of k-conservation selection rules indeed is negligible, as far as absorption is concerned. In emission this is definitely not the case, which is illustrated in Fig. 8, where the experimental and calculated $H0$-E_F separations are plotted versus carrier density. Experimentally, the $H0$-E_F separation is determined by taking the energy at the maximum in the polarization curve as the transition energy associated with $H0(k=0)$ to $E0(k=0)$ recombination,[32] and the half-maximum point at the high-energy side of the emission spectrum as due to $H0(k=k_F)$ or $L0(k=k_F)$ to $E0(k=0)$ recombination. The very favorable comparison with calculated

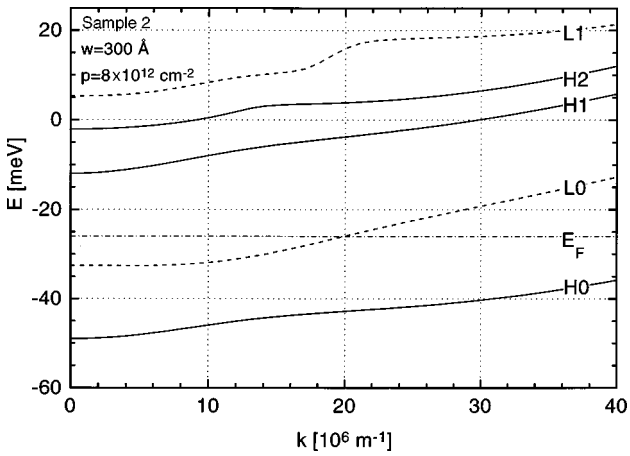

FIG. 9. Dispersion relations of the lowest subbands of sample 2. The solid and dashed lines denote heavy- and light-hole dispersions, respectively. The dash-dotted line indicates the position of the Fermi level E_F.

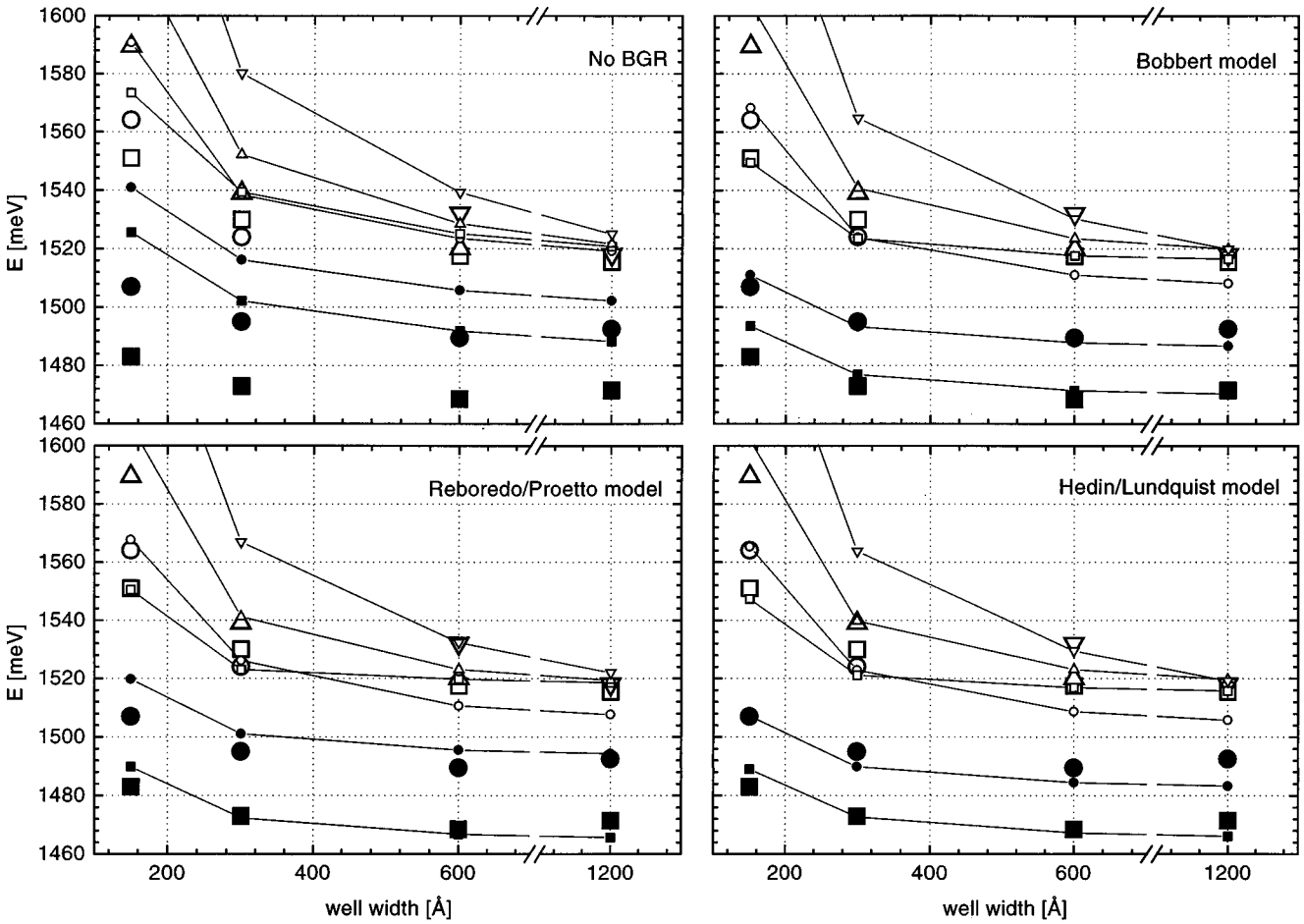

FIG. 10. Comparison of measured transition energies with calculated values, using various models for the hole exchange and correlation interactions discussed in the text, versus the width of the confining well. The large symbols denote experimental points, the small symbols denote calculations. The lines connect the calculated energies. The experimental error is usually less than 2 meV. The meaning of the symbols is as follows: solid squares, $H0$-$E0$; solid circles, $L0$-$E0$; open squares, $H2$-$E0$; open circles, $H1$-$E1$; open up triangle, $L1$-$E1$; open down triangle, $H2$-$E2$.

values shows that this assignment is correct, and that transitions in emission can either be direct or indirect in k. However, the maximum emission intensity still seems to arise from direct transitions, and positive and negative extrema in the polarization curve will in the following be assumed to indicate $H0(k=0)$ to $E0(k=0)$ and $L0(k=0)$ to $E0(k=0)$ transitions, respectively. It is worthwhile to point out that the onset of absorption does not correspond to $H0(k=k_F)$ or $L0(k=k_F)$ to $E0(k=k_F)$ transitions, as in most modulation-doped heterostructures, but to $H1$-$E1$ or $H2$-$E0$ transitions at the zone center. This is due to the large hole densities in the present samples, which cause extremely large Moss-Burstein shifts. As an example, the Moss-Burstein shifts for sample 3 are 56 meV for the $L0$-$E0$ transition, and more than 250 meV for the $H0$-$E0$ transition.

As a typical example, Fig. 9 shows the dispersion relation for the same sample as shown in Fig. 7 (no. 2), together with the calculated Fermi energy E_F. The well-known nonparabolicity of the valence-band states is apparently visible. However, extreme nonparabolicities as negative masses, which are generally found for the $L0$ band in heterostructures based on the $Al_xGa_{1-x}As$ system,[19] are absent. Nevertheless, the remaining nonparabolicities still strongly affect the optical spectra, which is manifested mainly in the nonstep-like behavior of the absorption spectra, see Fig. 7.

The summary of our experimental and numerical data is shown in Figs. 10 and 11, where measured and calculated transition energies are plotted versus the well width (Fig. 10) and the dopant concentration (Fig. 11). Experimental energies were determined at half height for steplike onsets, and at peak maximum for sharply peaked onsets. No correction for exciton binding energy has been applied, since the involved binding energies are relatively uncertain and small compared to the overall experimental error, see also the discussion in Sec. III B. Comparing the measured energies with the ones calculated without exchange and correlation corrections directly shows the need for these corrections, in contrast with the claim in Ref. 12. Furthermore, it shows that in these δ-doping layers the BGR cannot be accounted for by a rigid shift of all valence bands, like in, for instance, single quantum wells. Clear differences can also be found between the results obtained with the BGR models by Bobbert *et al.* and by Reboredo and Proetto, which both aim to account for the coexistence of light and heavy holes. These differences are most pronounced in the light-hole subbands, particularly at low doping concentrations and narrow well widths, cf. the

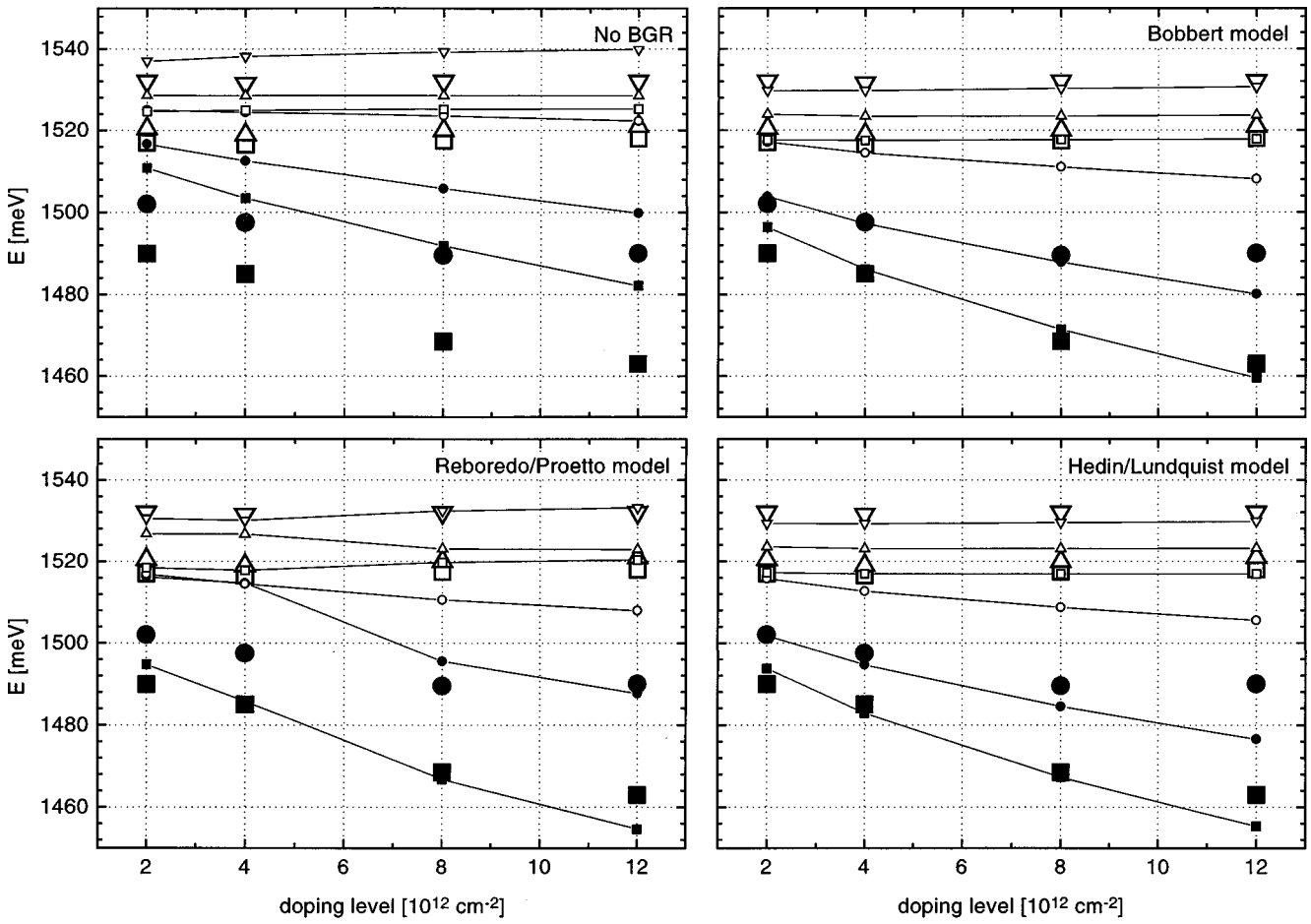

FIG. 11. As Fig. 10, but as a function of the total dopant concentration.

upper-right and lower-left panels of Figs. 10 and 11. Both the energies of the $L0$-$E0$ and $L1$-$E1$ transitions calculated with the Reboredo-Proetto model are far more than the experimental error of about 2 meV above the experimentally found values. Moreover, the Reboredo-Proetto model incorrectly predicts one occupied subband for a hole density of $p=4\times10^{12}$ cm^{-2}. A surprisingly good correspondence with experimental data is found when the one-particle model of Hedin and Lundqvist is used in the calculations. Comparing with the model by Bobbert *et al.* with ''fitting to the experimental data'' as criterion for success, the Bobbert model seems to prevail for all samples, except those with the lowest density and most narrow well width, for which the Hedin-Lundqvist model seems to prevail. The differences are, however, quite small. On physical grounds, the success of the model by Hedin and Lundqvist for p-type systems is accidental and based on a cancellation of errors,[1] to which we will come back in the next section.

V. DISCUSSION

A. Exchange and correlation

In the previous section, we have shown that the BGR model by Reboredo and Proetto systematically underestimates the renormalization of the light-hole-related transitions. These deviations are directly due to the fact that this model uses different exchange-correlation potentials for heavy and light holes, and that these potentials are only a function of the local density in the heavy- *or* light-hole subbands. The analogy with the spin-density functional formalism, on which this model is based, is tempting but invalid. The local ''heavy''- and ''light''-hole densities, obtained by Reboredo and Proetto from the envelope functions of the $|m_J|=\frac{3}{2}$ and $|m_J|=\frac{1}{2}$ spinor components, are easily shown to be dependent on the direction of the quantization axis, which, of course, should not be the case. Furthermore, the exchange and correlation interactions between ''light'' and ''heavy'' holes are, by definition, ignored in this model. Even in the hypothetical case of an infinitesimally small light-hole mass, when no states with $|m_J|=\frac{1}{2}$ are occupied, these interactions cannot be ignored due to the nondiagonal character of the Coulomb interaction with respect to the hole character.[1]

The surprisingly good correspondence between experimentally determined energies and those calculated with the Hedin-Lundquist model for exchange and correlation is, as stated above, due to a cancellation of errors. To be more precise, the implicit assumption that all holes are ''heavy,'' made by applying an ''electron gas'' model to a hole gas, leads to an overestimation of the exchange energy and an underestimation of the correlation energy. The qualitative reason why the exchange energy for the hole gas is smaller in magnitude than that for the electron gas is the fact that, besides the spatial degrees of freedom, there are four instead

of two internal degrees of freedom ($m_J = \pm\frac{3}{2}, \pm\frac{1}{2}$ for a hole gas, and only $_Jm = \pm\frac{1}{2}$ for an electron gas). Consequently, it is easier to fulfill the Pauli exclusion principle, which reduces the exchange interaction. The underestimation of the hole-correlation energy, when applying the Hedin-Lundquist model to a hole gas is also related to the number of internal degrees of freedom. Due to the coexistence of light and heavy holes, the number of possible excitations at the Fermi level is increased, leading to a higher dielectric constant for a hole gas than for an electron gas of the same density. A high dielectric constant means that the system reacts efficiently on a perturbation (strong screening), which implies a strong correlation with the perturbation. In this specific case the perturbation is just the Coulomb potential of any hole in the system. Therefore, the correlation energy of a system with four internal degrees of freedom is higher than that of a system with a lower degree of freedom.

The only method of defining local heavy- and light-hole fractions that is consistent with the LDA formalism is employed in the model by Bobbert *et al.* It states that, since LDA treats the quasi-2D charge distribution locally as a bulk density, also the bulk dispersion relations have to be used in determining the local heavy- and light-hole fractions. The success of the model of Bobbert *et al.* for the present samples therefore, mainly shows the validity of the local-density approximation in the calculation of the effects of hole exchange and correlation in quasi-2D systems of high degeneracy.

B. Exciton screening

The observation of strong excitonic features in the present, highly degenerate, samples may appear surprising at first sight. Although it is well known that the efficiency of Coulomb screening in 2D systems is strongly reduced as compared to that in 3D systems, straightforward extrapolation of available theoretical results to our samples suggests that only an infinitesimally small binding energy should remain.[33,34] However, as was pointed out in a few earlier publications,[35,8,9] standard 2D screening theory ignores the differences in probability distributions of various subbands along the growth direction. To be more specific, the relatively strong confinement of the occupied ground states ($H0$ and $L0$), leads to a poor screening of excitons formed by more extended states like $H2$ and $E0$.[35,8,9] Furthermore, it has been suggested[6] that the presence of ionized impurities inside the quantum well makes the screening of excitons less efficient, which will facilitate the survival of excitons up to the current doping concentrations. The overlap argument is in full agreement with the observation that no significant excitonic absorption enhancement is visible for the 150- and 300 Å wells. Due to the confinement by the $Al_{0.20}Ga_{0.80}As$ barriers, the extension of the $H2$ and $E0$ wave functions along the growth direction is not much larger than that of the $H0$ and $L0$ wave functions, causing a relatively efficient screening of the $H2$-$E0$ exciton.

There are two points that we would like to stress concerning the screening of excitons in these samples. The first is that it has been shown that peaked structures in absorption spectra are generally spoken an unreliable indicator for the presence or absence of excitons.[19,8] See, e.g., the peaks at 1540 and 1565 meV in the PLE spectra of the 300- and 150 Å wells, respectively [Figs. 7 and 4(a)], which can fully be accounted for by the valence-band structure only.[36] The absence of a peak in the absorption spectrum, on the other hand, does not imply the total bleaching of the exciton.[8] The second point, which is strongly related to this, is that we do not claim that, apart from the $H2$-$E0$ exciton, all excitons are unbound. The apparent dominance of the $H2$-$E0$ exciton in the spectra of wide wells is due to the subtle interplay between the exciton binding strength and the optical matrix element. The latter is extremely large for the $H2$-$E0$ transition in wide wells, as can directly be concluded from a comparison of the strengths of the $H0$-$E0$ and $H2$-$E0$ PL lines at 80 K, see Fig 6. As an example, the $H1$-$E1$ subbands are also expected to form an exciton of significant binding energy for wide wells ($w \geq 600$ Å), but the optical matrix element of $H1$-$E1$ transitions is at least a factor two smaller than that of the $H2$-$E0$ exciton for these well widths, which prevents the exciton from being identifiable in PLE.

C. The absence of a Fermi-edge singularity

In contrast to what is reported by Wagner and co-workers[11–13] for samples very similar to the ones discussed here, we do not find any indication for a Fermi-edge singularity in the PL spectra of our samples. It has been shown that such a FES can arise from either strong localization of the minority carriers[7,15,37–40] or a near-resonance condition between states at the Fermi level and those of a nearby excitonic level.[3,4,41–43] Due to the small electron mass in GaAs, the former condition is not very likely to be fulfilled, as was also noticed in Ref. 12. Furthermore, the small effective mass of the unlocalized electron will inhibit the observation of any FES-like features in emission spectra, due to the large recoil of the scattered electron.[4,14,15] The latter condition requires an excitonic level that is almost at resonance with the Fermi level. For all samples but the one with $p = 2\times10^{12}$ cm^{-2} the separation between E_F and the lowest occupied hole level is at least 13 meV, which is too far for causing any significant coupling in n-type systems.[41–44] For p-type systems, this is even more unlikely, which can be understood from a consideration of the lifetime broadening of the minority carriers γ. Apart from the separation between the Fermi level and the lowest unoccupied state γ is an essential parameter determining the strength of the FES.[43,4] In first order γ is proportional to the effective mass, leading to a smaller value for minority electrons than for minority holes, which, in turn, leads to a decrease of the FES intensity in p-type systems.[43] Moreover, it was shown by Rodriguez and Tejedor[4] that no such coupling at all can occur in symmetric potentials. Summarizing the above, the absence of a FES in the PL spectra of our samples appears to be in good agreement with most earlier work on the FES in emission spectra.

There are two significant differences between the present samples and the ones used by Wagner and co-workers. The first is the density range, which runs from 3×10^{12} to 4×10^{13} cm^{-2} in Refs. 12 and 13. However, the separations between E_F and the lowest unoccupied subband reported for these samples are of the same size as in our samples. The second, and probably most significant, difference concerns

the fact that Wagner and co-workers employ samples with a single δ-doped well. As was pointed out by Wagner *et al.*,[13] this might easily lead to a breaking of the symmetry of the confining potential, which can strongly enhance the formation of a FES.[4] Finally, we should stress that exciting above the band gap of the confining barriers did not, in any sense, change our spectra, in contrast to what is reported in Ref. 11.

It is interesting to mention the observation of a FES in a highly disordered system of Be-δ-doped bulk GaAs by Fritze *et al.*[7] In these samples, the extremely high Be coverage in the δ layer (up to 0.35 ML or $p=2.1\times10^{14}$ cm^{-2}) caused the formation of Be clusters. The resulting high disorder leads to the localization of the minority carriers (electrons), despite their low effective mass. The Be coverages used in our samples, maximally 0.02 ML, are far below the density at which the so-called surface phase transition occurs, and Be clusters start to form.

VI. CONCLUSIONS

Summarizing, we have studied many-body interactions in Be-δ-doped quantum wells, by means of a careful comparison between PL(E) experiments and self-consistent calculations. Different LDA models for the exchange and correlation potentials of an interacting hole gas have been compared with experiments. It is found that the model that was recently derived by Bobbert *et al.*[1] consistently describes the experimental band-gap renormalization, both for empty and filled subbands. Furthermore, our results indicate that ''heavy''- and ''light''-hole subbands experience the same exchange-correlation potential, which is consistent with the assumptions of the LDA formalism. For well widths above 600 Å a sharp peak dominates the absorption spectra of our samples, which is attributed to a $H2$-$E0$ exciton. The dominance of this exciton is explained in terms of a strong optical matrix element and a reduced screening efficiency of higher subbands, due to a small overlap with the screening particles. In contrast to earlier work on similar samples, no indication for a Fermi-edge singularity in PL was found, which is discussed and understood in the framework of other theoretical and experimental work on this singularity.

During the preparation of this manuscript, a paper was published by Enderlein *et al.*,[45] in which they theoretically discuss exchange and correlation interactions in degenerate p-type heterostructures. In this paper, a matrix expression on the Luttinger-Kohn basis is constructed for describing the exchange and correlation interactions. In spirit, this method differs significantly from the model proposed by Bobbert *et al.*[1] Moreover, one can show that the partial local heavy- and light-hole densities, as defined in this paper, do not add up to the total local-hole density. Therefore we stick to our conclusion that the model by Bobbert *et al.* is the only model that, within the LDA, consistently describes the effects of exchange and correlation.

[1] P. A. Bobbert, H. Wieldraaijer, R. van der Weide, M. Kemerink, P. M. Koenraad, and J. H. Wolter, Phys. Rev. B **56**, 3664 (1997).

[2] S. A. Brown, J. F. Young, Z. Wasilewski, and P. T. Coleridge, Phys. Rev. B **56**, 3937 (1997).

[3] S. J. Xu, S. J. Chua, X. H. Tang, and X. H. Zhang, Phys. Rev. B **54**, 17 701 (1996).

[4] F. J. Rodriguez and C. Tejedor, J. Phys.: Condens. Matter **8**, 1713 (1996).

[5] I. A. Buyanova, W. M. Chen, A. Henry, W.-X. Ni, G. V. Hansson, and B. Monemar, Phys. Rev. B **53**, 1701 (1996).

[6] A. C. Ferreira, P. O. Holz, B. E. Sernelius, I. Buyanova, B. Monemar, O. Mauritz, U. Ekenberg, M. Sundaram, K. Campman, J. L. Merz, and A. C. Gossard, Phys. Rev. B **54**, 16 989 (1996).

[7] M. Fritze, A. Kastalsky, J. E. Cunningham, W. H. Know, R. N. Pathak, and I. E. Perakis, Solid State Commun. **100**, 497 (1996).

[8] M. Kemerink, P. M. Koenraad, P. C. M. Christianen, R. van Schaijk, J. C. Maan, and J. H. Wolter, Phys. Rev. B **56**, 4853 (1997).

[9] M. Kemerink, P. M. Koenraad, A. Parlangeli, P. C. M. Christianen, R. van Schaijk, J. C. Maan, and J. H. Wolter, Phys. Status Solidi A **164**, 73 (1997).

[10] M. Kemerink, P. M. Koenraad, and J. H. Wolter, Phys. Rev. B **57**, 6629 (1998).

[11] J. Wagner, A. Ruiz, and K. Ploog, Phys. Rev. B **43**, 12 134 (1991).

[12] D. Richards, J. Wagner, H. Schneider, G. Hendorfer, M. Maier, A. Fischer, and K. Ploog, Phys. Rev. B **47**, 9629 (1993).

[13] J. Wagner, D. Richards, H. Schneider, A. Fischer, and K. Ploog, Solid-State Electron. **37**, 871 (1994).

[14] P. Hawrylak, Phys. Rev. B **44**, 3821 (1991).

[15] A. E. Ruckenstein and S. Schmitt-Rink, Phys. Rev. B **35**, 7551 (1987).

[16] Using the formula for the electrostatic potential of a charged plate $V=ped/2\epsilon_0\epsilon_1$, with d the separation between the topmost δ layer and the surface (600 Å), we find that 1.8×10^{12} cm^{-2} holes have to be transferred to surface states to overcome the mid-gap pinning of the Fermi level at the surface. So, even at the lowest doping concentration, the doping in the first δ layer is enough to accomplish this.

[17] M.-L. Ke, L. S. Rimmer, B. Hamilton, J. H. Evans, M. Missous, K. E. Singer, and P. Zalm, Phys. Rev. B **45**, 14 114 (1992).

[18] In fact, one should measure the integrated excitonic intensity. However, a large degree of arbitrariness exists in separating the excitonic and free-particle contributions to the total PLE spectrum, which makes a quantitative analysis along this line impossible. The followed method does not suffer from this problem.

[19] M. Kemerink, P. M. Koenraad, and J. H. Wolter, Phys. Rev. B **54**, 10 644 (1996).

[20] M. Kemerink, P. M. Koenraad, P. C. M. Christianen, A. K. Geim, J. C. Maan, J. H. Wolter, and M. Henini, Phys. Rev. B **53**, 10 000 (1996).

[21] *Physics of Group IV Elements and III-V Compounds*, edited by O. Madelung, M. Schultz, and H. Weiss, Landolt-Börnstein, New Series, Group III, Vol. 17, Pt. a (Springer-Verlag, Berlin, 1982); *ibid.*, Vol. 22, Pt. a (Springer-Verlag, Berlin, 1987).

[22] E. F. Schubert, J. M. Kuo, R. F. Kopf, H. S. Luftman, L. C. Hopkins, and N. J. Sauer, J. Appl. Phys. **67**, 1969 (1990).

[23] P. M. Koenraad, M. B. Johnson, H. W. M. Salemink, W. C. van der Vleuten, and J. H. Wolter, Mater. Sci. Eng., B **35**, 485 (1995).

[24] F. A. Reboredo and C. R. Proetto, Phys. Rev. B **47**, 4655 (1993).
[25] G. M. Sipahi, R. Enderlein, L. M. R. Scolfaro, and J. R. Leite, Phys. Rev. B **53**, 9930 (1996).
[26] L. Hedin and B. I. Lundqvist, J. Phys. C **4**, 2064 (1971).
[27] G. Tränkle, H. Leier, A. Forchel, H. Haug, C. Ell, and G. Weimann, Phys. Rev. Lett. **58**, 419 (1987).
[28] S. Haacke, R. Zimmermann, D. Bimberg, H. Kal, D. E. Mars, and J. N. Miller, Phys. Rev. B **45**, 1736 (1992).
[29] S. Das Sarma, R. Jalabert, and S.-R. E. Yang, Phys. Rev. B **41**, 8288 (1990).
[30] O. Gunnarsson and B. I. Lundqvist, Phys. Rev. B **13**, 4274 (1976).
[31] J. P. Pedrew and A. Zunger, Phys. Rev. B **23**, 5048 (1982).
[32] This is always a point of discussion. However, to get rid of the unpolarized bulk signal one has to look at the polarization of the PL signal. Under the reasonable assumptions that the electron distribution is (almost) thermalized and that k-conserving transitions are more efficient than non-k-conserving ones, the extrema in the polarization will correspond to transitions at $k=0$, independent of a slight (in)homogeneous broadening.
[33] G. D. Sanders and Y.-C. Chang, Phys. Rev. B **35**, 1300 (1987).
[34] D. A. Kleinman, Phys. Rev. B **32**, 3766 (1985).
[35] A. B. Henriques, Phys. Rev. B **44**, 3340 (1991).
[36] Peaked structures can arise in absorption spectra due to an anticrossing in the corresponding valence-band state. E.g., the $L1$-$E1$ transition in Fig. 7 is allowed for small k. At $k=10\times10^6$ m (Fig. 9) L1 experiences an anticrossing with a higher subband, which changes the character of the $L1$ subband, and makes the $L1$-$E1$ transition parity forbidden, resulting in a sudden drop of the PLE signal.
[37] Y. H. Zhang, N. N. Ledentsov, and K. Ploog, Phys. Rev. B **44**, 1399 (1991).
[38] M. S. Skolnick, J. M. Rorison, K. J. Nash, D. J. Mowbray, P. R. Tapster, S. J. Bass, and A. D. Pitt, Phys. Rev. Lett. **58**, 2130 (1987).
[39] G. Livescu, D. A. B. Miller, D. S. Chemla, M. Ramaswamy, T. Y. Chang, N. Sauer, A. C. Gossard, and J. H. English, IEEE J. Quantum Electron. **QE-24**, 1677 (1988).
[40] S. Schmitt-Rink, C. Ell, and H. Haug, Phys. Rev. B **33**, 1183 (1986).
[41] W. Chen, M. Fritze, W. Walecki, A. V. Nurmikko, D. Ackley, J. M. Hong, and L. L. Chang, Phys. Rev. B **45**, 8464 (1992).
[42] M. Fritze, W. Chen, A. V. Nurmikko, J. Jo, M. Santos, and Shayegan, Phys. Rev. B **45**, 8408 (1992).
[43] J. F. Mueller, Phys. Rev. B **42**, 11 189 (1990).
[44] P. Hawrylak, Phys. Rev. B **44**, 6262 (1991).
[45] R. Enderlein, G. M. Sipahi, L. M. R. Scolfaro, and J. R. Leite, Phys. Rev. Lett. **79**, 3712 (1997).